Appl. Chem. Eng., Vol. 31, No. 5, October 2020, 539-544
https://doi.org/10.14478/ace.2020.1065

Article

고성능 전기 화학 pH 센서를 위한 유연한 3차원 다공성 폴리아닐린 필름 제조

박홍준 · 박승화 · 김호준 · 이경균*,† · 최봉길†

강원대학교 화학공학과, *나노종합기술원
(2020년 8월 18일 접수, 2020년 9월 4일 수정, 2020년 9월 4일 채택)

Preparation of Flexible 3D Porous Polyaniline Film for High-Performance Electrochemical pH Sensor

Hong Jun Park, Seung Hwa Park, Ho Jun Kim, Kyoung G. Lee*,†, and Bong Gill Choi†

Department of Chemical Engineering, Kangwon National University, Samcheok 25913, Republic of Korea
**Nano-Bio Application Team, National Nanofab Center (NNFC), Daejeon 34141, Republic of Korea*
(Received August 18, 2020; Revised September 4, 2020; Accepted September 4, 2020)

초 록

본 연구에서는 넓은 면적의 나노필라 배열 필름을 기반으로 포토 및 소프트 리소그래피 기술과 화학적 희석 고분자 중합을 조절하여 3차원 다공성의 폴리아닐린 필름을 제조하였다. 3차원 폴리아닐린 필름은 계층 간 연결된 폴리아닐린 나노파이버들로 구성되어 있어, 넓은 표면적과 개방형의 다공성 구조를 가지는 3차원 계층형 나노웹 필름을 형성한다. 전기화학분석법을 기반으로 3차원 폴리아닐린 필름이 유연한 pH 센서 전극이 되는 것을 증명하였다. 3차원 폴리아닐린 필름은 이상적인 네른스트 거동과 근접한 60.3 mV/pH의 높은 민감도를 보였다. 또한, 3차원 폴리아닐린 전극은 10 min의 빠른 반응 속도, 우수한 반복성 그리고 높은 선택성을 나타내었다. 3차원 폴리아닐린 전극을 기계적으로 굽힌 상태에서 센서 특성을 측정하였을 때, 전극이 60.4 mV/pH의 높은 민감도를 보여줌으로써, 유연한 pH 센서 성능을 증명하였다.

Abstract

A three-dimensional (3D) porous polyaniline (PANI) film was fabricated by a combined photo-and soft-lithography technique based on a large-area nanopillar array, followed by a controlled chemical dilute polymerization. The as-obtained 3D PANI film consisted of hierarchically interconnected PANI nanofibers, resulting in a 3D hierarchical nanoweb film with a large surface and open porous structure. Using electrochemical measurements, the resulting 3D PANI film was demonstrated as a flexible pH sensor electrode, exhibiting a high sensitivity of 60.3 mV/pH, which is close to the ideal Nernstian behavior. In addition, the 3D PANI electrode showed a fast response time of 10 s, good repeatability, and good selectivity. When the 3D PANI electrode was measured under a mechanically bent state, the electrode exhibited a high sensitivity of 60.4 mV/pH, demonstrating flexible pH sensor performance.

***Keywords**: pH sensor, Polyaniline, Electrochemistry, 3D structure, Potentiometry*

1. Introduction

A quantitative analysis of alkalinity and acidity in solutions is essential in laboratories and industries to ensure the quality and safety of products and processes[1-3]. The pH of a solution is determined using various capacitive, chemiresistive, luminescence, optical, and potentiometric techniques[4-9]. Among them, potentiometric sensors are widely used because of their simple structure, easy operation, and low-cost fabrication. Potentiometric sensors measure the open-circuit potential between a pH-sensitive (working) electrode and a reference electrode[10-14]. pH monitoring of human body fluids (e.g., sweat, tear, saliva, and urine) has a great potential for diagnosis and self-health care because changes in pH are significantly related to various diseases, such as cystic fibrosis, ocular rosacea, gingivitis, and nephrolithiasis[15-19]. In addition, wearable sensor systems based on non-invasive, continuous, and real-time monitoring methods are shifting the current hospital and clinical paradigms towards individual

† Corresponding Author: K. G. Lee: Kangwon National University, Department of Chemical Engineering, Samcheok 25913, Republic of Korea; B. G. Choi: National Nanofab Center (NNFC), Nano-Bio Application Team, Daejeon 34141, Republic of Korea
Tel:+82-33-570-6545 e-mail: K. G. Lee: kglee@nnfc.re.kr; B. G. Choi: bgchoi@kangwon.ac.kr

pISSN: 1225-0112 eISSN: 2288-4505

health management, also known as smart mobile healthcare[20-22].

In this regard, conventional glass-type and solution-filled pH sensors have been transformed into miniaturized, flexible, and solid-state pH sensors that can be more suitable for wearable sensor applications [23-25]. To modify conventional pH sensors, numerous metal oxides and conducting polymers have been explored as pH-sensitive materials, including IrOx, RuO_2, MnO_2, TiO_2, SnO_2, polyaniline, polypyrrole, and polyethyleneimine[26-32]. As a state-of-the-art electrode material, iridium oxide-based pH sensors show near- or super-Nernstian responses (> 60 mV/pH) over a wide pH range, good stability, and fast response time[26,33-35]. However, the preparation of iridium oxide electrodes requires a thermal oxidation process at a temperature above 500 ℃, and expensive raw materials limit their usage in pH sensor applications[26]. Compared to metal oxides, conducting polymers, particularly polyaniline, are easy to synthesize, mechanically flexible, and relatively inexpensive[14,31,32]. Polyaniline-based materials are sensitive to different pH levels due to their oxidation and reduction reactions with hydronium ions[37]. Recent reports describe that nanostructured electrode materials, compared to their counterpart bulk materials, have enhanced electrochemical sensing performance because of their large surface area, which can enhance charge transfer[38].

In this study, we developed a simple and scalable method for the fabrication of 3D porous PANI films with a hierarchical nanoweb morphology. The unique structure of the PANI film was prepared by a combined photo- and soft-lithography technique based on a large-area nanopillar array, followed by controlled dilute polymerization. The deposition of PANI nanofibers onto the nanopillar surface resulted in a 3D hierarchical nanoweb film with a large surface and open porous structure. The resulting PANI film was demonstrated as a flexible pH sensor electrode using electrochemical measurements, showing a high sensitivity of 60.3 mV/pH, a fast response time of 10 s, good repeatability, and good selectivity.

2. Experimental

2.1. Materials

Ammonium persulfate (98%), aniline (99.5%), hydrochloric acid, calcium chloride, magnesium chloride, ammonium chloride, and potassium chloride were purchased from Sigma-Aldrich (USA). Perchloric acid (70%) was purchased from Junsei (Japan). The pH buffer solutions (pH 4.0, 5.0, 6.0, 7.0, 8.0, 9.0, 10.0, 11.0, 12.0, and 13.0) were purchased from Samchun Chemicals (Korea). Deionized water (18.2 M · cm) was employed in all experiment.

2.2. Fabrication of 3D PANI electrode

Prior to preparing the 3D PANI electrode, a Si nanohole master mold was prepared as follows: A Si wafer was placed in a furnace to induce surface oxidation of the SiO_2 layer. The thermally oxidized wafer was then spin-coated with a photoresist to form a dot-patterned array. The obtained array wafer was etched by inductively coupled plasma (ICP, TCP9400SE, Lam Research, United States) with a gas blend of Cl_2, HBr, and O_2 to form a Si nanohole master mold. To prepare the nanopillar array film, a mixture of polyurethane (MINS-311RN, Munuta Tech) and NOA63 (Norland Optical Adhesives) was spin-coated onto the Si master mold. After UV-induced polymerization and curing treatment, the polyurethane and NOA63 (PUN) film was peeled off from the Si master mold. For the uniform and fine-controlled synthesis of PANI nanofibers onto the nanopillar array, gold/titanium (Au/Ti) was coated onto the PUN film using a photolithography technique. The Au/Ti/PUN nanostructured film was immersed in a solution of 1 M $HClO_4$, 6 mM ammonium persulfate, aniline, and deionized water, in which the concentration of aniline monomer was 18 mM. Dilute polymerization of the aniline was performed at 3 ℃ while incubating for 24 h. The obtained 3D PANI electrode was rinsed with deionized water and washed with ethanol several times.

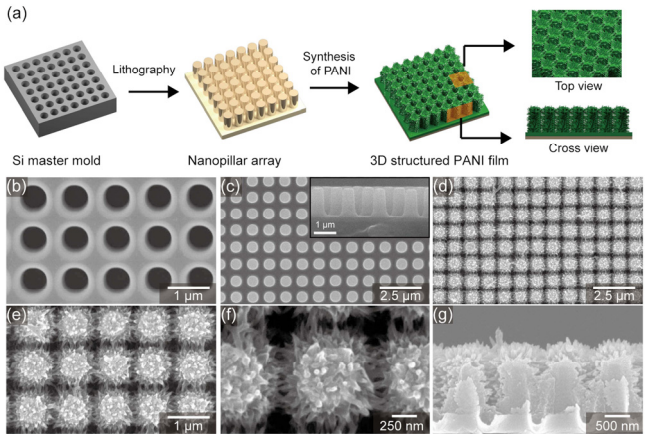

Figure 1. (a) A schematic image for fabrication process of 3D PANI electrode and the SEM images of (b) Si mold, (c) PUN nanopillar, (d,e,f) top and (g) cross sectional views for 3D PANI structure.

2.3. Characterization

Scanning electron microscopy (SEM) images were obtained using a field emission scanning electron microscope (S-4800). Fourier transform infrared (FT-IR) spectra were collected on a JASCO FT-IR 4600. Each spectrum was recorded from 4000 to 400 cm^{-1}. Electrochemical characterization was measured by using an Iviumstat (USA). All electrochemical measurements were performed at room temperature, and the obtained data were within the error range of ± 1%. The sensitivity, limit of detection (LOD), response time, repeatability, selectivity, and durability test were performed using an open-circuit potential technique.

3. Results and Discussion

Figure 1a shows the experimental procedure of the fabrication of the 3D flexible PANI film via preparation of a polymeric nanopillar array film, followed by chemically dilute polymerization of aniline monomer onto the nanopillar surface. The one-dimensional (1D) ordered nanopillar array film was prepared by a combined photo- and soft-lithography process using a silicon hole mold (Figure 1a). The PUN solution was filled in a silicon mold (Figure 1b), followed by UV-curing, and finally the 1D nanopillar array film was peeled off from the mold. The

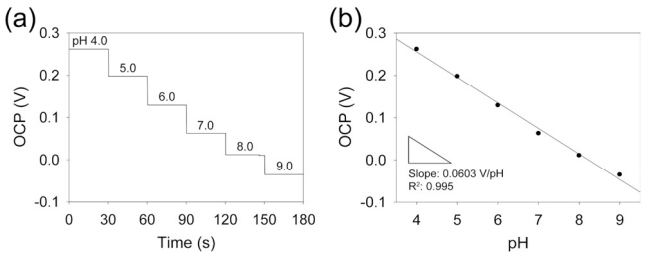

Figure 2. The OCP measurements recorded for increasing the pH level (a) and the calibration plot (b) of OCP versus pH in the pH 4.0~9.0 range.

as-obtained nanopillar array of PUN film shows a highly ordered 1D array structure (Figure 1c). The dilute polymerization method enabled the synthesis and growth of PANI nanofibers onto the nanopillar surface, resulting in a 3D interconnected structure (Figure 1d and 1e). The surface and cross-sectional SEM images (Figure 1f and 1e) revealed that the 3D hierarchical pore structure was formed from the bottom to the top surfaces. This 3D continuous and open pore structure is favorable for the charge transfer process, enhancing electrochemical performance.

The pH sensing performance of the 3D PANI film was evaluated by potentiometric measurements. A two-electrode configuration was employed with the 3D PANI film as the working electrode and Ag/AgCl as the reference electrode. The potentiometric technique measures the change in the open-circuit potential (OCP) between the two electrodes at different pH levels. Figure 2a shows the OCP responses of the 3D PANI electrode with solutions of pH 4~9. The calibration curve in Figure 2b exhibits a linear slope of 60.3 mV/pH with R^2 = 0.995 in the pH range of 4~9. The OCP responses follow the Nernstian equation[39,40]:

$$E = E^o + 2.303RT/nF(\mathrm{pH}) = E^o - 0.059\mathrm{pH} \quad (1)$$

where E is the electrode potential (mV), E^o is the standard electrode potential, R is the gas constant (8.314 J/K・mol), T is the absolute temperature (K), n is the number of electron transfers, and F is the Faraday constant (96485 C/mol). Based on IUPAC recommendations, the limit of detection was calculated from the intersection of the two lines, and found to be pH 12.1 (Figure 3a). The response time of the pH sensors was evaluated by alternately dipping the 3D PANI electrode in solutions of pH 4 and 6 without the washing and conditioning steps (Figure 3b). The response time was determined when $\triangle E/\triangle t$ reached 1 mV/min, as suggested by the IUPAC method[39, 40]. The 3D PANI electrode showed a fast response (saturated) time of 10 s, and after 10 s, stable OCP signals were observed.

To further demonstrate the electrochemical performance of the 3D PANI electrode, its reversibility was evaluated by measuring its OCP responses in acid-to-base-to-acid solutions (Figure 3c). The 3D PANI electrode exhibited same slopes of 60.1 and 59.8 mV/pH for the forward and reverse directions, respectively. During the titration measurements, the OCP responses were almost maintained in both directions.

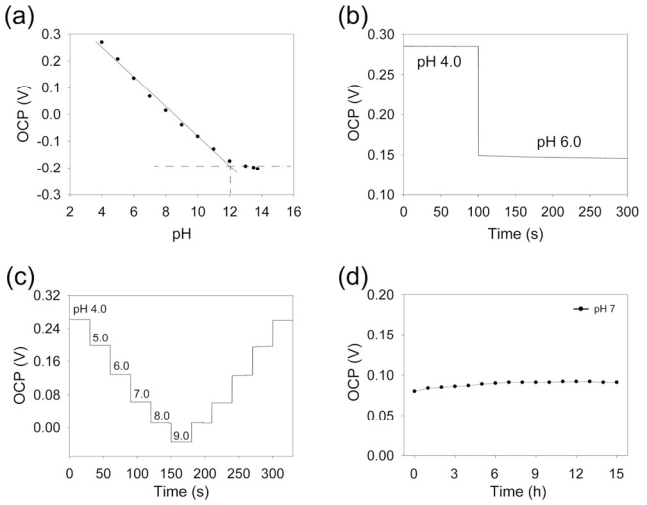

Figure 3. (a) The limit of detection curve of the 3D PANI electrode, conditioned in solution of pH 4.0, (b) the EMF responses for the 3D PANI electrode when changing from pH 4.0 to 6.0, (c) A repeatability for the 3D PANI electrode in pH 4~9, (d) long-term stability for the 3D PANI electrode for 15 h in pH 7.

These results indicate that the 3D PANI electrode has good reversibility. The drift of pH sensors is one of the most important factors for the durability of pH sensors. If the pH electrode has been dried or may not have been properly conditioned, the OCP signals drift, especially during long periods of measurement. To demonstrate its durability, the OCP response of the 3D PANI electrode immersed in pH 7 solution was measured for 15 h (Figure 3d). The 3D PANI electrode exhibited a low potential drift of 0.7 mV/h, which is much lower than those of other previously reported PANI electrodes[9]. The most important characteristic of a potentiometric pH sensor is the ability to selectively measure a primary ion (H^+) over other interfering ions present in the solution. The selectivity coefficient of the pH sensor was investigated by the separate solution method (SSM) recommended by IUPAC. To evaluate the selectivity coefficients of the pH sensor, the OCP responses were measured for the primary ion (H^+) in the solution and compared with the responses for interfering ions including Na^+, K^+, NH_4^+, Ca^{2+}, and Mg^{2+}. The selectivity coefficient (K) can be calculated by SSM using the following equation[39,40]:

$$\triangle E = E_J - E_I = \frac{RTln10}{zF}\left\{\frac{Z_I - Z_J}{Z_J}\log C + \log K_{IJ}^{pot}\right\} \quad (2)$$

where I is the primary ion and J is the interfering ion, E is the experimentally measured EMF value of the pH sensor, R is the gas constant (8.314 J/mol・K), T is the absolute temperature, F is the Faraday constant (96485 C/mol), z is the charge number, and C is the concentration of primary ion. Based on the IUPAC recommended SSM, the obtained selectivity coefficients (K) for the pH sensor are shown in Table 1. A K value equal to 1.0 means that the pH sensor responds equally to the primary ion (H^+) as well as interfering ions. The 3D PANI-based pH sensor shows K values smaller than 1.0, indicating

Table 1. Selective Coefficients of 3D PANI Sensor Obtained by a Separation Solution Method (SSM) for Primary ion (H^+) against Na^+, K^+, NH_4^+, Ca^{2+}, and Mg^{2+} (Interference Ions)

Ion (J)	$\log K_{IJ}^{POT}$	K_{IJ}^{POT}
Na^+	-8.9	1.3×10^{-9}
K^+	-7.2	7.0×10^{-8}
NH_4^+	-6.7	1.9×10^{-7}
Ca^{2+}	-10.4	4.1×10^{-11}
Mg^{2+}	-10.7	2.3×10^{-11}

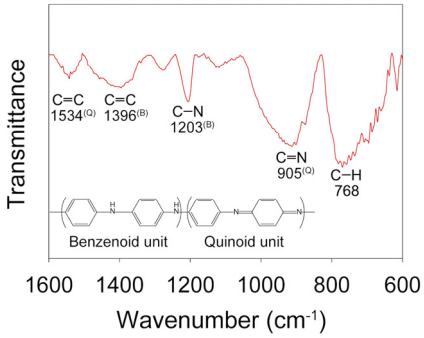

Figure 4. FT-IR spectra of the 3D PANI electrode.

that the pH sensor can accurately measure H_3O^+ over interfering ions. The superior sensing performance of the 3D PANI film originates from the intrinsic redox reactions of PANI in the presence of hydronium ions in solution. To confirm the successful synthesis of PANI on the Au/Ti pillar, Fourier transform infrared (FT-IR) spectroscopy was used, as shown in Figure 4. The prominent peaks of the PANI electrode at 1534, 1396, 1203, 905, and 768 cm^{-1} are attributed to the C=C stretching in the quinoid ring, C=C stretching in the benzenoid ring, C-N stretching in the benzenoid ring, C-N stretching in the quinoid ring, and C-H out of plane bending[9,41].

The flexibility of the 3D PANI electrode for pH sensing was further investigated by measuring the OCP responses of the electrode in a mechanically bent state. Figure 5a shows a photograph of the bent 3D PANI electrode with a bending radius of 0.25 mm. The bent 3D PANI electrode exhibited stable OCP responses at pH levels of 4, 5, 6, 7, 8, and 9 (Figure 5b). The slope of the calibration curve of the bent 3D PANI electrode was calculated to be 60.3 mV/pH. This value is consistent with that of the mechanically normal 3D PANI electrode (60.4 mV/pH) (Figure 5c). This result is attributed to the excellent mechanical stability of the 3D PANI electrode.

4. Conclusion

This study demonstrated the application of a 3D porous film, composed of hierarchically interconnected PANI nanofibers, as a pH sensor electrode. The 3D PANI electrode was fabricated by a combined photo- and soft-lithography technique, followed by controlled dilute polymerization. The PANI material could detect changes in pH, via redox reactions with hydronium ions. The 3D porous architecture of the

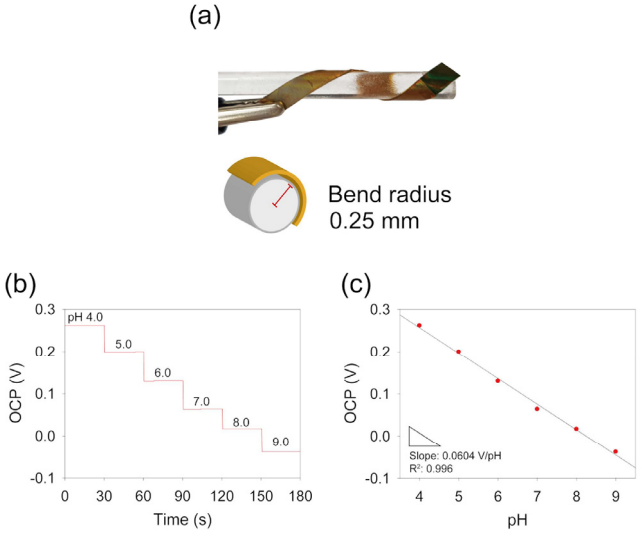

Figure 5. (a) Photography of a bent 3D PANI electrode, (b) OCP responses of 3D PANI electrode with different pH levels, and (c) calibration curve of bent 3D PANI electrode with increasing pH level.

PANI electrode resulted in a high sensitivity of 60.3 mV/pH, which is close to ideal Nernstian behavior. In addition, the 3D PANI electrode showed a fast response time of 10 s, good repeatability, and good selectivity. When the 3D PANI electrode was measured under a mechanically bent state, the electrode exhibited a high sensitivity of 60.4 mV/pH, demonstrating flexible pH sensor performance. The excellent pH sensing performance and flexibility of the 3D PANI electrode could lead to its use for wearable pH sensor applications.

Acknowledgment

This work was supported by the National Research Foundation of Korea (NRF) Grant funded by the Korean Government (MSIP) (No. 2018R1A2A3075668).

References

1. J. H. Yoon, S. B. Hong, S. Yun, S. J. Lee, T. J. Lee, K. G. Lee, and B. G. Choi, High performance flexible pH sensor based on polyaniline nanopillar array electrode, *J. Colloid Interface Sci.*, **490**, 53-58 (2017).
2. J. H. Yoon, K. H. Kim, N. H. Bae, G. S. Sim, Y. Oh, S. J. Lee, T. J. Lee, K. G. Lee, and B. G. Choi, Fabrication of newspaper-based potentiometric platform for flexible and disposable ion sensors, *J. Colloid Interface Sci.*, **508**, 167-173 (2017).
3. S. Islam, H. Bakhtiar, S. Naseem, M. S. B. A. Aziz, N. Bidin, S. Riaz, and J. Ali, Surface functionality and optical properties impact of phenol red dye on mesoporous silica matrix for fiber optic pH sensing, *Sens. Actuators A, Phys.*, **276**, 267-277 (2018).
4. K. Hammarling, M. Engholm, H. Andersson, M. Sandberg, and H. Nilsson, Broad-range hydrogel-based pH sensor with capacitive readout manufactured on a flexible substrate, *Chemosensors*, **6**, 30 (2018).
5. S. Chinnathambi and G. J. W. Euverink, Polyaniline functionalized

electrochemically reduced graphene oxide chemiresistive sensor to monitor the pH in real time during microbial fermentations, *Sens. Actuators B, Chem.*, **264**, 38-44 (2018).
6. S. Hou, J. Dong, M. Tang, X. Jiang, Z. Jiao, and B. Zhao, Triple-interpenetrated lanthanide-organic framework as dual wave bands self-calibrated pH luminescent probe, *Anal. Chem.*, **91**, 5455-5460 (2019).
7. Y. Zhao, M. Lei, S. Liu, and Q. Zhao, Smart hydrogel-based optical fiber SPR sensor for pH measurements, *Sens. Actuators B, Chem.*, **261**, 226-232 (2018).
8. M. Pospíšilová, G. Kuncová, and J. Trögl, Fiber-optic chemical sensors and fiber-optic bio-sensors, *Sensors*, **15**, 25208-25259 (2015).
9. H. J. Park, J. H. Yoon, K. G. Lee, and B. G. Choi, Potentiometric performance of flexible pH sensor based on polyaniline nanofiber arrays, *Nano Converg.*, **6**, 9 (2019).
10. H. J. Park, J. Jeong, J. H. Yoon, S. G. Son, Y. K. Kim, D. H. Kim, K. G. Lee, and B. G. Choi, Preparation of ultrathin defect-free graphene sheets from graphite via fluidic delamination for solid-contact ion-to-electron transducers in potentiometric sensors, *J. Colloid Interface Sci.*, **560**, 817-824 (2020).
11. S. G. Son, H. J. Park, Y. K. Kim, H. Cho, and B. G. Choi, Fabrication of low-cost and flexible potassium ion sensors based on screen printing and their electrochemical characteristics, *ACS Appl. Chem. Eng.*, **30**, 737-741 (2019).
12. J. H. Yoon, S. Kim, Y. Eom, J. M. Koo, H. Cho, T. J. Lee, K. G. Lee, H. J. Park, Y. K. Kim, H. Yoo, S. Y. Hwang, J. Park, and B. G. Choi, Extremely fast self-healable bio-based supramolecular polymer for wearable real-time sweat-monitoring sensor, *ACS Appl. Mater. Interfaces*, **11**, 46165-46175 (2019).
13. J. H. Yoon, H. J. Park, S. H. Park, K. G. Lee, and B. G. Choi, Electrochemical characterization of reduced graphene oxide as an ion-to-electron transducer and application of screen-printed all-solid-state potassium ion sensors, *Carbon Lett.*, **30**, 73-80 (2020).
14. A. U. Alam, Y. Qin, S. Nambiar, J. T. W. Yeow, M. M. R. Howlader, N. Hu, and M. J. Deen, Polymers and organic materials-based pH sensors for healthcare applications, *Prog. Mater. Sci.*, **96**, 174-216 (2018).
15. W. P. Nikolajek, and H. M. Emrich, pH of sweat of patients with cystic fibrosis, *Klin. Wschr.*, **54**, 287-288 (1976).
16. M. B. Abelson, A. A. Sadun, I. J. Udell, and J. H. Weston, Alkaline tear pH in ocular rosacea, *Am. J. Ophthalmol.*, **90**, 866-869 (1980).
17. K. Chaisiwamongkhol, C. Batchelor-Mcauley, and R. G. Compton, Amperometric micro pH measurements in oxygenated saliva, *Analyst*, **142**, 2828-2835 (2017).
18. S. Baliga, S. Muglikar, and R. Kale, Salivary pH: A diagnostic biomarker, *J. Indian Soc. Periodonto.*, **17**, 461-465 (2013).
19. T. Kwong, C. Robinson, D. Spencer, O. J. Wiseman, and F. E. K. Frankl, Accuracy of urine pH testing in a regional metabolic renal clinic: Is the dipstick accurate enough? *Urolithiasis*, **41**, 129-132 (2013).
20. J. H. Yoon, S. Kim, H. J. Park, Y. K. Kim, D. X. Oh, H. Cho, K. G. Lee, S. Y. Hwang, J. Park, and B. G. Choi, Highly self-healable and flexible cable-type pH sensor for real-time monitoring of human fluids, *Biosens. Bioelectron.*, **150**, 111946 (2020).
21. J. Ding and W. Qin, Recent advances in potentiometric biosensors, *Trends Anlyt. Chem.*, **124**, 115803 (2020).
22. A. J. Bandodkar and J. Wang, Non-invasive wearable electrochemical sensors: A review, *Trends Biotechnol.*, **32**, 363-371 (2014).
23. L. Manjakkal, S. Dervin, and R. Dahiya, Flexible potentiometric pH sensors for wearable systems, *RSC Adv.*, **10**, 8594-8617 (2020).
24. M. Parrilla, I. Ortiz-Gómez, R. Cánovas, A. Salinas-Castillo, M. Cuartero, and G. A. Crespo, Wearable potentiometric ion patch for on-body electrolyte monitoring in sweat: Toward a validation strategy to ensure physiological relevance, *Anal. Chem.*, **91**, 8644-8651 (2019).
25. Y. Qin, H. Kwon, M. M. R. Howlader, and M. J. Deen, Microfabricated electrochemical pH and free chlorine sensors for water quality monitoring: Recent advances and research challenges, *RSC Adv.*, **5**, 69086-69109 (2015).
26. W. Huang, H. Cao, S. Deb, M. Chiao, and J. C. Chiao, A flexible pH sensor based on the iridium oxide sensing film, *Sens. Actuators A, Phys.*, **169**, 1-11 (2011).
27. Y. Liao and J. Chou, Preparation and characteristics of ruthenium dioxide for pH array sensors with real-time measurement system, *Sens. Actuators B, Chem.*, **128**, 603-612 (2008).
28. L. Telli, B. Brahimi, and A. Hammouche, Study of a pH sensor with MnO_2 and montmorillonite-based solid-state internal reference, *Solid State Ion.*, **128**, 225-259 (2000).
29. Y. Liao and J. Chou, Preparation and characterization of the titanium dioxide thin films used for pH electrode and procaine drug sensor by sol-gel method, *Mater. Chem. Phys.*, **114**, 542-548 (2009).
30. C. Tsai, J. Chou, T. Sun, and S. Hsiung, Study on the time-dependent slow response of the tin oxide pH electrode, *IEEE Sens. J.*, **6**, 1243-1249 (2006).
31. B. Lakard, G. Herlem, S. Lakard, R. Guyetant, and B. Fahys, Potentiometric pH sensors based on electrodeposited polymers, *Polymer*, **46**, 12233-12239 (2005).
32. K. Shiu, F. Song, and K. Lau, Effects of polymer thickness on the potentiometric pH responses of polypyrrole modified glassy carbon electrode, *J. Electroanal. Chem.*, **476**, 109-117 (1999).
33. P. Marsh, L. Manjakkal, X. Yang, M. Huerta, T. Le, L. Thiel, J. C. Chiao, H. Cao, and R. Dahiya, Flexible iridium oxide based pH sensor integrated with inductively coupled wireless transmission system for wearable applications, *IEEE Sens. J.*, **20**, 5130-5138 (2020).
34. S. Shahrestani, M. C. Ismail, S. Kakooei, M. Beheshti, M. Zabihiazadboni, and M. A. Zavareh, Iridium oxide pH sensor based on stainless steel wire for pH mapping on metal surface, *IOP Conf. Ser. Mater. Sci. Eng.*, **328**, 012014 (2018).
35. M. Tabata, C. Ratanaporncharoen, A. Asano, Y. Kitasako, M. Ikeda, T. Goda, A. Matsumoto, J. Tagami, and Y. Miyahara, Miniaturized Ir/IrOx pH sensor for quantitative diagnosis of dental caries, *Procedia Eng.*, **168**, 598-601 (2016).
36. M. T. Ghoneim, A. Nguyen, N. Dereje, J. Huang, G. C. Moore, P. J. Murzynowski, and C. Dagdeviren, Recent progress in electrochemical pH-sensing materials and configurations for biomedical applications, *Chem. Rev.*, **119**, 5248-5297 (2019).
37. T. Lindfors, and A. Ivaska, pH sensitivity of polyaniline and its substituted derivatives, *J. Electroanal. Chem.*, **531**, 43-52 (2002).
38. S. H. Park, J. Jeong, S. J. Kim, K. H. Kim, S. H. Lee, N. H. Bae, K. G. Lee, and B. G. Choi, Large-area and 3D polyaniline nanoweb film for flexible supercapacitors with high rate capability and long cycle life, *ACS Appl. Energy Mater.*, DOI: 10.1021/acsaem.0c01140 (2020).
39. R. P. Buck and E. Lindner, Recommendations for nomenclature of ion-selective electrodes (IUPAC recommendations 1994), *Pure*

Appl. Chem., **66**, 2527-2536 (1994).
40. J. M. Pingarrón, J. Labuda, J. Barek, C. M. A. Brett, M. F. Camões, M. Fojta, and D. B. Hibbert, Terminology of electrochemical methods of analysis (IUPAC recommendations 2019), *Pure Appl. Chem.*, **92**, 641-694 (2020).
41. H. Noby, A. H. El-Shazly, M. F. Elkady, and M. Ohshima, Novel preparation of self-assembled HCl-doped polyaniline nanotubes using compressed CO_2-assisted polymerization, *Polymer*, **156**, 71-75 (2018).

Authors

Hong Jun Park; Master Course, Researcher, Department of Chemical Engineering, Kangwon National University, Samcheok 25913, Republic of Korea; qkrghdwnssl@gmail.com

Seung Hwa Park; Master Course, Researcher, Department of Chemical Engineering, Kangwon National University, Samcheok 25913, Republic of Korea; fairi1220@gmail.com

Ho Jun Kim; Undergraduate Student, Researcher, Department of Chemical Engineering, Kangwon National University, Samcheok 25913, Republic of Korea; gokhj9963@gmail.com

Kyoung G. Lee; Ph.D., Senior Researcher, Nano-Bio Application Team, National Nanofab Center (NNFC), Daejeon 34141, Republic of Korea; kglee@nnfc.re.kr

Bong Gill Choi; Ph.D., Associate Professor, Department of Chemical Engineering, Kangwon National University, Samcheok 25913, Republic of Korea; bgchoi@kangwon.ac.kr